Supplementary Material (ESI) for Chemical Communications

Supplementary Information†

Highly-efficient solution-processed OLEDs based on new bipolar emitters

Ming Zhang, Shanfeng Xue, Wenyue Dong, Qi Wang, Teng Fei, Cheng Gu, and Yuguang Ma*

State Key Laboratory of Supramolecular Structure and Materials, Jilin University,

2699 Qianjin Avenue, Changchun, 130012, P. R. China.

1. General Details

All manipulations involving air-sensitive reagents were performed under an atmosphere of dry nitrogen. All reagents, unless otherwise specified, were obtained from Aldrich, Acros and TCI Chemical Co. and used as received. All the solvents used were further purified before use. Infrared (IR) spectra were recorded on a Perkin-Elmer spectrophotometer in the 400-4000 cm^{-1} region, using a powdered sample on a KBr plate. The ^{1}H-NMR spectra were recorded on AVANCZ 500 spectrometers at 298 K by utilizing deuterated chloroform as solvent and tetramethylsilane (TMS) as standard. Ultraviolet-visible (UV-vis) absorption spectra were recorded on a model UV-3100 spectrophotometer. Fluorescence spectra (77K) were performed using a model RF-5301PC spectrophotometer.

The fabrication and measurements of OLEDs are as following: ITO-coated glass with a sheet resistance of <50 Ω^{-1} was used as the substrate. The substrate was patterned to give an effective device size of 4 mm^2. The pretreatment of ITO includes a routine chemical cleaning using detergent，iso-propylalcohol, acetone, toluene, deionized water in sequence in sequence. For spin-coating devices, PEDOT:PSS was coated from water dispersion on ITO substrate with a speed of 1500 rpm at room temperature, yielding a 70 nm thick layer after drying (ca. 105 °C; 5 min), subsequently the active layer from chloroform solutions containing 10 mg/mL **TCDqC**, **TCBzC** and **TCNzC** (3000 rpm) for single-layer and 10 mg/ml TCDqC, 20 mg/ml **TCBzC** and 20 mg/ml TCNzC, (3000rpm) chloroform solutions for double-layer spin-coating onto the PEDOT at room temperature. And then a shadow was used to define the deposition areas for the metal cathodes. Finally, for the single layer devices, the Ba (10 nm) and Al cathode (100 nm) were in order thermally evaporated onto the emitting-layers in vacuum with a base pressure of 5×10^{-4} Pa; For the double layer devices, the electron-transporting materials TPBI [2, 2', 2" - (1, 3, 5 - Benzinetriyl) - tris (1 - phenyl -1 - H -benzimidazole)] (30-60 nm), LiF (0.5 nm) and Al cathode (100 nm) were in order thermally

evaporated onto the emitting-layers in vacuum with a base pressure of 5×10^{-4} Pa. Electroluminescence (EL) spectra and the corresponding Commission Internationale del'Eclairage (CIE) coordinates were measured by a PR-650 spectra-scan spectrometer. The brightness-current-voltage characteristics were recorded simultaneously with the measurement of the EL spectra by combining the spectrometer with a Keithley 2400 programmable electrometer. All measurements were carried out at room temperature under ambient conditions.

2. Synthesis and Characterization

The Suzuki coupling reactions between M2 and 1, 1-dibromodibenzo [*f*, *h*] quinoxaline (**DBQ**), 2, 1, 3-benzothiadiazole (**BTZ)** and 2, 1, 3-naphthothiadiazole (**NTZ**) were performed to yield the RGB materials of **TCDqC**, **TCBzC** and **TCNzC**. **M1**, [1] **DBQ**, [2] **BTZ** [3] and **NTZ** [4] were prepared by following the published procedures. Fig. S1 is the synthesis of the key monomer **M2**. The following is the synthesis of **M2** and the RGB materials

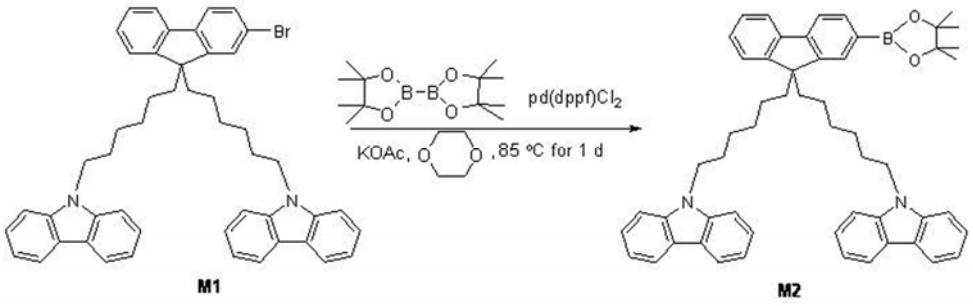

Fig S1 The synthesis of the monomer **M2.**

M2: A solution of 9, 9'-(6 ,6'-(2-bromo-9*H*-fluorene-9, 9-diyl)bis(hexane-6, 1-diyl))bis (9*H*-carbazole) (2.0 g), 4, 4, 4', 4' ,5 ,5 ,5' ,5' -octamethyl- 2, 2' - bi (1, 3, 2 -dioxaborolane)(1.54 g), $Pd(dppf)Cl_2$ (104 mg), and KOAc(1.45 g) in degassed 1,4-dioxane(15 mL) was stirred at 80 °C for 1 d. The reaction was quenched by adding water, and the resulting mixture was washed with dichloromethane. The organic layers were collected, dried with anhydrous magnesium sulphate, and concentrated in vacuum. It was then purified via silica gel chromatography by petroleum ether: dichloromethane = 3:2 to give the desired compound as a white solid in 80% yield (1.70 g). ^{1}H NMR (500 MHz, $CDCl_3$)：δ (ppm) 8.07-8.06 (d, J = 7.3 Hz, 4H), 7.82-7.80 (d, J = 7.3 Hz, 1H), 7.71-7.68 (m, 3H), 7.44-7.40 (m, 4H), 7.32-7.27 (m, 5H), 7.24-7.23 (d, J = 5.5 Hz, 2H), 7.22-7.28 (m, 4H), 4.16-4.13 (m, 4H), 1.97-1.86 (m, 4H), 1.68-1.62 (m, 4H), 1.36 (s, 12H), 1.15-1.00 (m, 8H), 0.61-1.47 (m, 4H).

TCDqC: 1,1-dibromodibenzo[*f*, *h*]quinoxaline (**DBQ**) (82.1 mg) and 9,9'-(6, 6'-(2-(4,4, 5,5-tetramethyl-1,3, -dioxaborolan-2-yl)-9*H*-fluorene-9,9-diyl)bis(hexane-6,1-diyl))bis(9*H*-carbazole) (332.5 mg) were dissolved in freshly distilled tetrhydrofuran (6 mL) under nitrogen. Potassium carbonate 2 M in water (1 mL) was added, together with ethanol (0.2 mL). The mixture was cooled in liquid nitrogen and thoroughly degassed. And them tetrakis(triphenylphosphine) palladium(0) (18.0 mg) was added and the resulting mixture was vigorously stirred at 75 °C for 2 d. After cooling to room temperature, dichloromethane was added and the water phase was extracted. The organic phase was collected and dried with anhydrous magnesium sulphate. After evaporation of the solvent, the residue was purified via chromatography by petroleum ether: dichloromethane = 1: 2. The desired compound was obtained in 78 % yield (255.1 mg). Solution photoluminescence quantum yield is 53 % (in THF, quinine sulfate as standard). ^{1}H NMR (500 MHz, DMSO-d6)**:** δ (ppm) 9.46 (s, 1H), 9.04 (s, 1H), 8.97-8.95 (d, J = 8.8 Hz, 1H), 8.26-8.24 (d, J = 7.3 Hz, 1H), 8.05-8.03 (d, J = 7.6 Hz, 4H), 7.96-7.94 (d, J = 8.2 Hz, 1H), 7.91 (s, 1H), 7.89-7.87 (d, J = 7.6 Hz, 1H), 7.84-7.83 (d, J= 6.7 Hz, 1H), 7.44-7.42 (d, J = 8.5 Hz, 4H), 7.34-7.31 (m, 6H), 7.28-7.25 (m, 1H), 7.10-7.07 (m, 4H), 4.24-4.21 (m, 4H), 2.06-1.84 (m, 4H), 1.55-1.53 (m, 4H), 1.04 (s, 8H), 0.58-0.46 (m, 4H). ^{13}C NMR ($CDCl_3$, 125 MHz): δ (ppm) 151.70, 151.12, 143.47, 141.95, 141.38, 141.20, 141.10, 140.72, 139.65, 130.72, 130.09, 129.40, 127.72, 127.41, 126.91, 125.90, 123.91, 123.23, 123.11, 121.94, 120.65, 120.38, 119.02, 108.99, 55.57, 43.29, 40.68, 30.02, 29.10, 27.17, 24.00. FT-IR (KBr, cm^{-1}): 3050, 2928, 2850, 1598, 1486, 1455, 1326, 1229, 1150, 1000, 818, 745, 723. MALDI-TOF-MS: *m/z* 1556.12 $[M+H]^+$ 1555.9. Anal. Calcd. for $C_{114}H_{102}N_6$: C, 87.99; H, 6.61; N, 5.40. Found: C, 87.76; H, 6.86; N, 5.18.

TCBzC: Simlar to **TCDqC**. yield: 71 %. Solution photoluminescence quantum yield is 35 % (in THF, quinine sulfate as standard). ^{1}H NMR (500 MHz, DMSO): δ 8.045 (d, 8H), 8.003 (s, 2H), 7.953 (m, 4H), 7.888 (s, 2H), 7.847 (d, 2H), 7.398 (d, 8H), 7.329-7.278 (m, 14H), 7.075 (t, 8H), 4.181 (t, 8H), 1.946 (d, 8H), 1.043 (m, 16H), 0.852 (m, 8H), 0.588 (m, 8H). ^{13}C NMR ($CDCl_3$, 125 MHz): δ (ppm) 154.65, 151.34, 151.11, 141.73, 141.07, 140.74, 136.65, 133.78, 128.66, 128.27, 127.81, 127.44, 125.91, 124.22, 123.26, 123.14, 120.68, 120.47, 120.23, 119.04, 108.99, 55.49, 43.28, 40.64, 30.13, 29.14, 27.21, 24.10. FT-IR (KBr, cm^{-1}): 3046, 2930, 2853, 1594, 1482, 1464, 1451, 1322, 1230, 1175, 1155, 1121, 1069, 1007, 956, 902, 846, 789, 758, 722, 699, 639, 583, 536, 482, 426. MALDI-TOF-MS: *m/z* 1462.2 $[M+H]^+$ 1461.98. Anal. Calcd. for $C_{104}H_{96}N_6S$: C, 85.44; H, 6.62; N, 5.75. Found: C, 85.28; H, 6.95; N, 5.56.

TCNzC: Similar to **TCDqC.** yield: 62 %. Solution photoluminescence quantum yield is 42 % (in THF, rhodamine as standard). ^{1}H NMR (500 MHz, DMSO-d6): δ (ppm) 8.13-7.94 (5H), 7.94-7.86

(1H), 7.86-7.76 (1H), 7.52-7.20 (13H), 7.14-7.96 (5H), 4.36-4.05 (5H), 1.95-1.72 (5H), 1.66-1.47 (5H), 1.20-0.91 (10H). ^{13}C NMR ($CDCl_3$, 125 MHz): δ (ppm) 151.99, 151.27, 150.82, 141.57, 141.16, 140.76, 135.60, 132.39, 131.09, 130.54, 127.86, 127.51, 126.73, 126.54, 125.93, 123.28, 123.17, 120.71, 120.48, 120.23, 119.07, 109.02, 55.48, 43.32, 40.55, 30.21, 29.20, 27.30, 24.27, 24.15. FT-IR (KBr, cm^{-1}): 3048, 2934, 2846, 1593, 1484, 1451, 1327, 1231, 1151, 1119, 1000, 924, 868, 810, 745, 725, 698, 640, 577, 517, 459. MALDI-TOF-MS: m/z 1512.7 (calcd.1512.04). Anal. Calcd for $C_{108}H_{98}N_6S$: C, 85.79; H, 6.53; N, 5.56. Found: C, 85.81; H, 6.41; N, 5.65.

3. The TGA and DSC properties

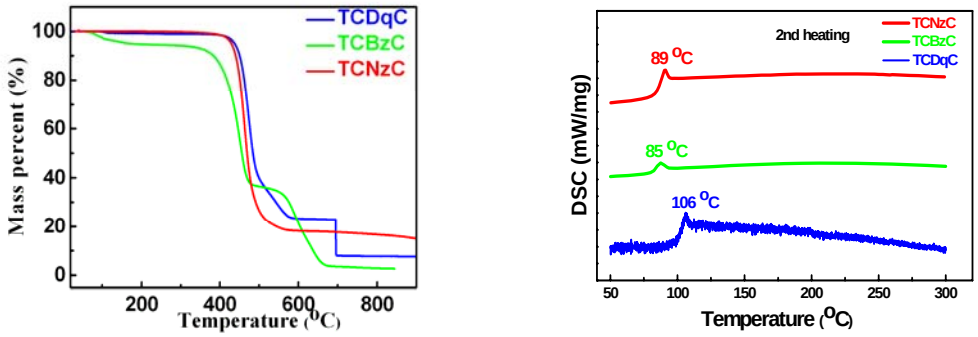

(a) **(b)**

Fig S2 The TGA (a) and DSC (b) Curves of the **TCDqC**, **TCBzC** and **TCNzC**

Fig S2 is the TGA and DSC spectra of the three compounds. As can be seen, the three materials are thermally stable with 5 % weight loss up to 400 °C under nitrogen, indicating of good thermal stability. Taking **TCBzC** as an example, it involves the loss of 68% of the mass of the sample to 416 °C. This stage is ascribed to the loss of the side chains of the compound. The second weight loss step starts at 565 °C and can be assigned to the decomposition of the backbone.

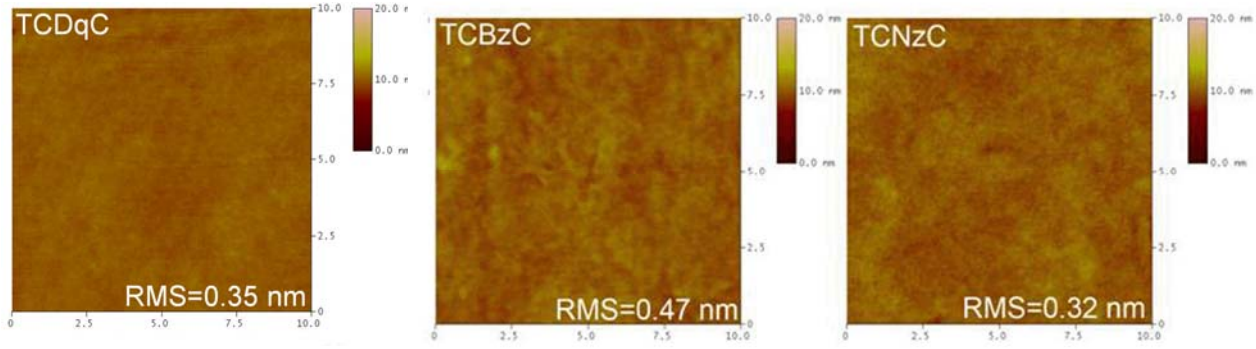

Fig. S3 The AFM images of the **TCBzC** and **TCNzC**

4. The AFM images

Fig S3 is the AFM images of **TCDqC**, **TCBzC** and **TCNzC** films. It can be seen that the spin coating films have a fairly smooth surface morphology with a root mean square (rms) roughness of 0.35 nm, 0.47 nm and 0.32 nm for **TCBzC** and **TCNzC**, respectively.

5. The photophysical properties

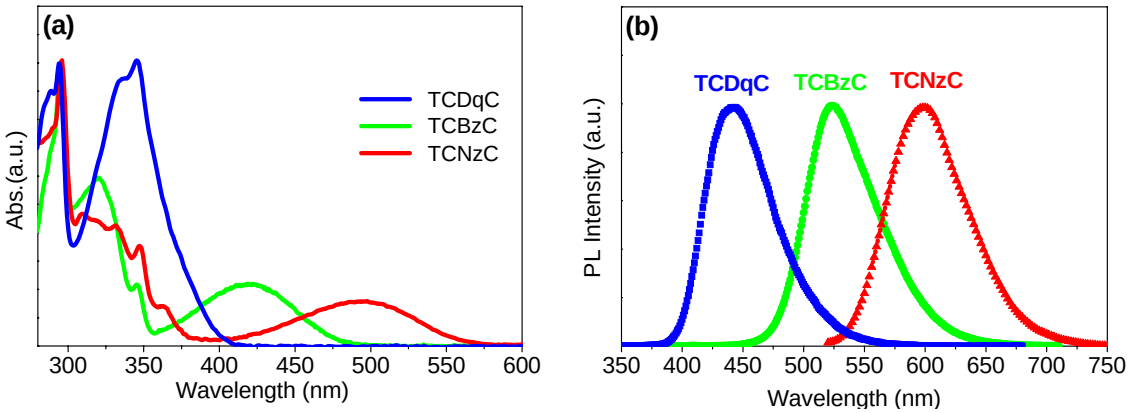

Fig S4 The absorption and PL spectra of the **TCDqC**, **TCBzC** and **TCNzC** in THF.

Fig S4a shows the absorption spectra of **TCDqC**, **TCBzC** and **TCNzC** in dilute tetrahydrofuran (THF) (ca. 1.0×10^{-4} M). Taking **TCBzC** as an example, the absorption spectrum of **TCBzC** in THF solution has four absorption peaks of 263, 294, 320 and 419 nm, respectively. The low-energy band around 419 nm is attributed to the absorption of narrow band-gap **BTZ** unit. The band around 320 nm, which is similar to that observed for other fluorene-based oligomers, and attributed to π–π* electronic transitions in the fluorene backbone. The 263 nm and 294 nm high-energy bands are attributed to transitions in the peripheral carbazole groups. The absorption spectra for the films show similar peaks as that in THF solution.

Fig. S4b shows the PL spectra of the **TCDqC**, **TCBzC** and **TCNzC** in tetrahydrofuran. As can be seen, **TCDqC**, **TCBzC** and **TCNzC** exhibit blue, green and red emission with the $\lambda_{max\ PL}$ at 441, 524 and 598 nm, respectively, which should be due to changing the electron injection units of the rigid core. Except the corresponding RGB emission, there is no emission from the peripheral carbazole groups and fluorene units in the backbone.

5. The EL properties

Fig. S5 is the EL spectra of the single-layer and double-layer device based on **TCDqC**, **TcBzC** and **TCNzC**, respectively, which are similar. The double-layer device structure is ITO/PEDOT:PSS/ **TCDqC** or **TCNzC (spin-coating)**/TPBi(30-60nm) /LiF(0.5nm)/Al(100nm). Here, **TPBi** functions

as hole-blocking layer and electron-transport layer, which might help balance the hole and electron injection and transport.

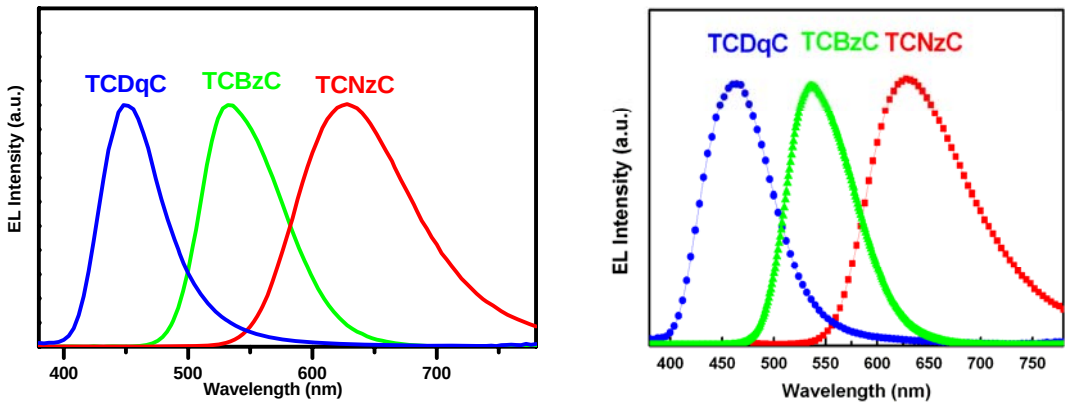

(a) (b)

Fig. S5 The EL spectra of the **TCDqC**, **TCBzC** and **TCNzC** single layer (a) and double layer (b) devices

Fig. S6 is the EL properties of **TCDqC** and **TCNzC**, respectively. The **TCDqC** spin-coating double-layer device exhibited a maximum brightness of 3280 cd m^{-2}, luminous efficiency of 3.7 cd A^{-1} and power efficiency of 1.7 lm W^{-1} shown in Fig. S7a. The **TCNzC** spin-coating film double-layer device exhibits a maximum brightness of 1136 cd m^{-2}, luminous efficiency of 7.2 cd A^{-1} and power efficiency of 2.3 lm W^{-1}, shown in Fig.S7b. Compared with those of the single-layer devices, the performances were significantly improved.

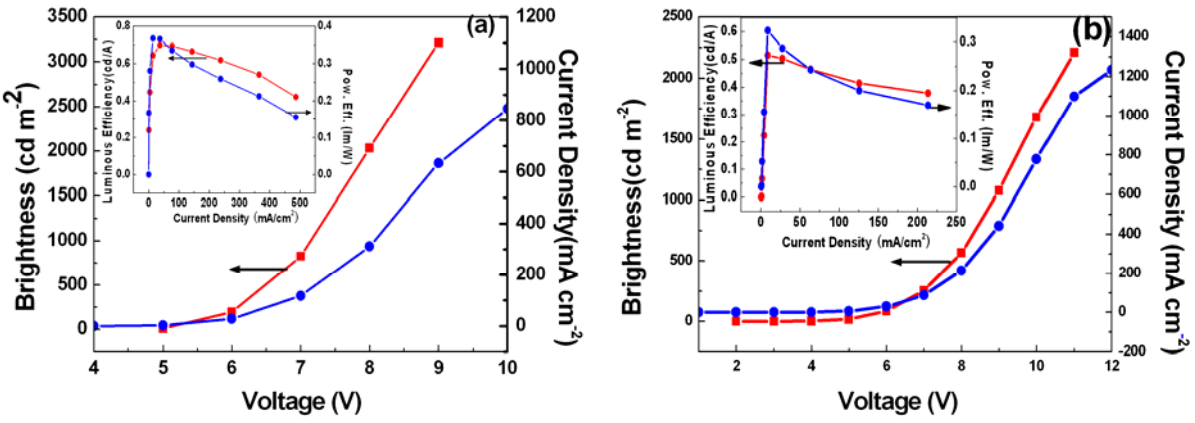

Fig. S6 (a) The voltage- luminance- current density characteristics of **TCDqC** spin-coating single-layer device. The inset shows the current-density-luminance-efficiency-power-efficiency characteristics. (b) The voltage-luminance- current density characteristics of **TCNzC** spin-coating single-layer device. The inset shows the current density-luminance efficiency-power efficiency characteristics.

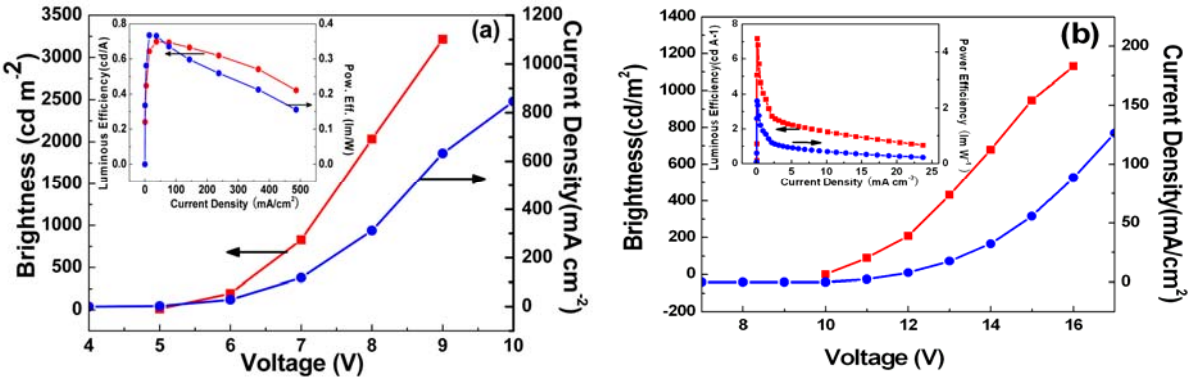

Fig. S7 The voltage-luminance- current-density characteristics of spin-coating double-layer device based on **TCDqC** (a) and **TCNzC** (b), respectively. The inset shows the current density-luminance efficiency-power efficiency characteristics.

Reference:

1. S. Tang, M. Liu, P. Lu, H. Xia, M. Li, Z. Q. Xie, F. Z. Shen, C. Gu, H. Wang, B. Yang, Y. Ma, *Adv. Funct. Mater.*, 2007, **17**, 2869.
2. E. J. Foster, R. B. Jones, C. Lavigueur, V. E. Williams, *J. Am. Chem. Soc.* 2006, **128**, 8569.
3. M. Zhang, H. N. Tsao, W. Pisula, C. Yang, A. K. Mishra, K. Müllen, *J. Am. Chem. Soc.*, 2007, **129**, 3472.
4. P. Wei, L. Duan, D-Q. Zhang, J. Qiao, L. Wang, R. Wang, G. Dong, Y. Qiu, *J. Mater. Chem.*, 2008, **18**, 806.